ACS SyntheticBiology

pubs.acs.org/synthbio Research Article

Red-Light-Induced Genetic System for Control of Extracellular Electron Transfer

Fengjie Zhao, Christina M. Niman, Ghazaleh Ostovar, Marko S. Chavez, Joshua T. Atkinson, Benjamin M. Bonis, Jeffrey A. Gralnick, Mohamed Y. El-Naggar, and James Q. Boedicker*

Cite This: *ACS Synth. Biol.* 2024, 13, 1467−1476 Read Online

ACCESS | Metrics & More | Article Recommendations | Supporting Information

ABSTRACT: Optogenetics is a powerful tool for spatiotemporal control of gene expression. Several light-inducible gene regulators have been developed to function in bacteria, and these regulatory circuits have been ported to new host strains. Here, we developed and adapted a red-light-inducible transcription factor for *Shewanella oneidensis*. This regulatory circuit is based on the iLight optogenetic system, which controls gene expression using red light. A thermodynamic model and promoter engineering were used to adapt this system to achieve differential gene expression in light and dark conditions within a *S. oneidensis* host strain. We further improved the iLight optogenetic system by adding a repressor to invert the genetic circuit and activate gene expression under red light illumination. The inverted iLight genetic circuit was used to control extracellular electron transfer within *S. oneidensis*. The ability to use both red- and blue-light-induced optogenetic circuits simultaneously was also demonstrated. Our work expands the synthetic biology capabilities in *S. oneidensis*, which could facilitate future advances in applications with electrogenic bacteria.

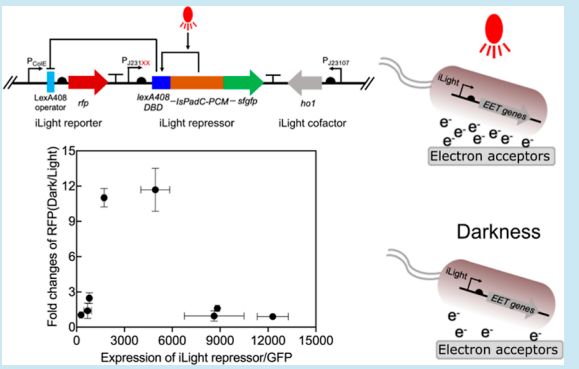

KEYWORDS: *Shewanella oneidensis MR-1, optogenetics, red light, cytochromes, extracellular electron transfer, electrochemical measurements*

INTRODUCTION

Optogenetics combines light-sensitive proteins and genetic techniques to control cellular processes within living organisms.[1] Synthetic optogenetic circuits can be constructed to tune gene expression with light-responsive transcription factors.[1] In recent years, optogenetic circuits have been developed to control gene expression in bacteria in response to illumination with blue, green, red, or near-infrared light.[2−7] Optogenetic circuits have been utilized to control gene expression to regulate many microbial processes, such as biochemical production,[8−11] biofilm formation,[12,13] and bacterial infection.[14] Although optogenetics has been implemented in model bacteria, such as *Escherichia coli*,[6,12] *Bacillus subtilis*,[15] and *Pseudomonas aeruginosa*,[14,16] there is still a need to extend these systems to other hosts for specific microbial processes.

Shewanella oneidensis MR-1 is a model electroactive organism, whose extracellular electron-transfer (EET) pathways have been well studied.[17,18] EET within *S. oneidensis* MR-1 utilizes a network of multiheme *c*-type cytochromes to route electrons from the cellular interior to external electron acceptors.[19−24] Synthetic biology strategies have been developed to regulate the EET capabilities of *S. oneidensis*, such as using genetic circuits to control the genes encoding the multiheme *c*-type cytochromes of the EET pathway. West et al., developed a native inducible system to tune the expression level of one multiheme cytochrome−porin complex (MtrCAB) to control EET capabilities.[25] In another study, clustered regularly interspaced short palindromic repeats interference (CRISPRi) and small regulatory RNA (sRNA) were used to repress the transcription and translation of *mtrA* to regulate EET efficiency.[26] Recently, Dundas et al., developed chemically induced transcriptional logic gates to control the EET flux of *S. oneidensis* by tuning the transcription and translation of EET-related genes.[27] A plasmid toolkit with different promoters and replication origins was characterized and utilized to control cytochrome expression in *S. oneidensis* for EET regulation.[28] The EET pathway of *S. oneidensis* has also been reconstructed successfully in *E. coli* through heterologous expression of the related genes encoding the *c*-type cytochromes.[29,30] Despite these advances in establishing synthetic biology approaches in *S. oneidensis*, the use of

Received: November 14, 2023
Revised: April 15, 2024
Accepted: April 16, 2024
Published: May 2, 2024

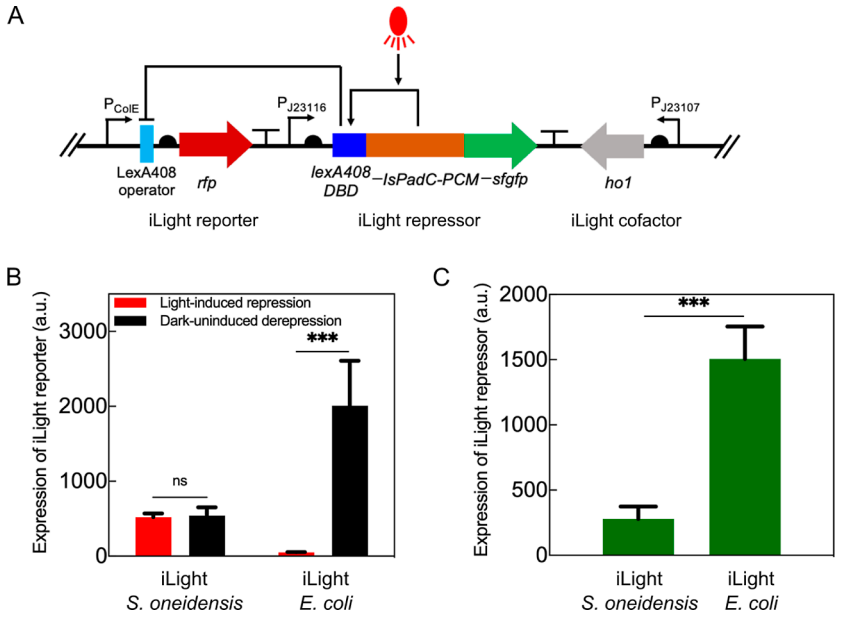

Figure 1. Characterization of the iLight genetic circuit in *S. oneidensis* and *E. coli*. (A) Single plasmid iLight genetic circuit contained iLight repressor, iLight reporter, and iLight cofactor. The RFP reporter measures light-regulated gene expression and sfGFP measures the expression level of the iLight repressor. (B) RFP fluorescence intensity measurements of iLight reporter expression in *S. oneidensis* and *E. coli* cultured under red light and dark conditions, respectively. $p = 0.7462$ for *S. oneidensis* light vs *S. oneidensis* dark and $p = 0.0006$ for *E. coli* light vs *E. coli* dark (two-tailed unpaired *t*-test). (C) GFP fluorescence intensity measurements of iLight repressor expression in *S. oneidensis* and *E. coli*. $p = 0.0005$ for *S. oneidensis* vs *E. coli* (two-tailed unpaired *t*-test). The measurements (mean ± SD) were derived from triplicate experiments. a.u., arbitrary units. Significance is indicated as $***p < 0.001$ and ns (not significant) $p > 0.05$.

optogenetic gene circuits to control EET has not been implemented.

S. oneidensis can transfer electrons through cytochromes on the nanometer scale and can also form living conductive biofilms for long-distance electron transport across neighboring cells on the micrometer scale.[31−33] We previously developed a lithographic strategy to pattern conductive biofilms of *S. oneidensis*, using the blue-light-induced genetic circuit pDawn to control cell aggregation.[34] This technique enabled tunable current generation by varying the dimensions of the electroactive biofilms. Since our previous work showed the potential of using optogenetics to pattern electrogenic microbes on the micrometer scale, adapting additional optogenetic systems for *S. oneidensis* could enable new strategies to control EET and develop advanced living electronics.[32]

A recently published paper developed a single-component red-light-induced optogenetic system, named iLight, for transcriptional regulation in *E. coli*.[35] We developed and adapted this iLight optogenetic system into *S. oneidensis* using a thermodynamic model to inform promoter engineering. Then we improved the iLight optogenetic system by introducing a genetic inverter to activate the gene expression using red light in *S. oneidensis*. Finally, we used this iLight genetic circuit to control the expression of cytochromes and regulate the EET activity of *S. oneidensis*. Our work demonstrated a new circuit to control gene expression in *S. oneidensis* using red light and demonstrated light-induced EET activity of *S. oneidensis*.

RESULTS

Importing the iLight Optogenetic System to *S. oneidensis*. The iLight optogenetic system was originally developed and optimized in *E. coli*.[35] It consists of a plasmid that encodes a light-sensitive repressor. The repressor is a chimeric protein containing a LexA408 DNA-binding domain fused to a photosensory domain IsPadC-PCM and sfGFP, henceforth referred to as "iLight repressor". An RFP reporter gene is regulated by the iLight repressor (Figure 1A). The proposed mechanism of action for the iLight optogenetic system is that red light induces tetramerization of the iLight photosensory module, which enables the LexA408 DNA-binding domains to form active transcription factor dimers.[35] The iLight photosensory module requires the tetrapyrrole biliverdin IXα (BV) as the chromophore to enable the light-responsive function of the iLight repressor (Figure S1). In our system, the *ho1* gene, a heme oxygenase from *Synechocystis* sp. PCC6803,[5] is expressed from the iLight plasmid for BV synthesis (Figure 1A).

We then tested this single plasmid iLight genetic circuit in *E. coli* and *S. oneidensis*. In *E. coli*, RFP fluorescence measurements confirmed that the iLight genetic circuit repressed the expression of the RFP reporter gene under the illumination of red light (Figure 1B). When cultured in the dark, the RFP expression was derepressed, resulting in a 40-fold increase in RFP expression (Figure 1B). However, in *S. oneidensis* transformed with the iLight plasmid, the expression level of the RFP reporter was similar in both cells cultured in red light and in the dark (Figure 1B). To determine if this circuit failure was caused by limited expression of the iLight repressor in a new host, we measured expression using sfGFP fusion to iLight. The expression level of the iLight repressor in *S. oneidensis* was much lower than in *E. coli* (Figure 1C). We hypothesized that the low expression of the iLight repressor could be the reason the iLight genetic circuit did not result in light-regulated gene expression in *S. oneidensis*.

Adjusting the Expression Level of the iLight Repressor. The expression of the iLight repressor was much lower in *S. oneidensis* than in *E. coli*, suggesting that differential

https://doi.org/10.1021/acssynbio.3c00684
ACS Synth. Biol. 2024, 13, 1467−1476

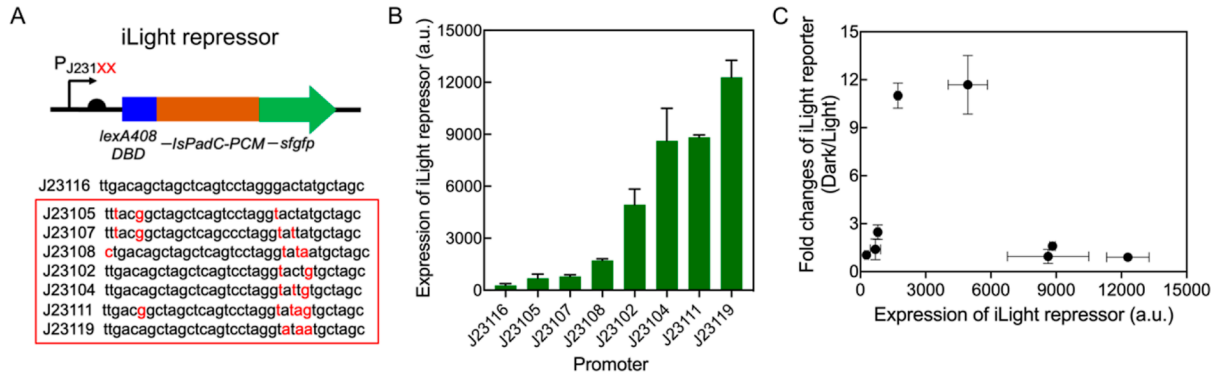

Figure 2. Adapting the iLight optogenetic system for *S. oneidensis*. (A) Site-directed mutagenesis of the promoter to tune expression of the iLight repressor. (B) Expression of the iLight repressor in *S. oneidensis* from these promoters, as measured via expression of cotranscribed sfGFP. (C) Fold changes of the iLight reporter (dark/red light) in *S. oneidensis* strains containing different promoters of the iLight repressor. The measurements (mean ± SD) were derived from triplicate experiments. a.u., arbitrary units.

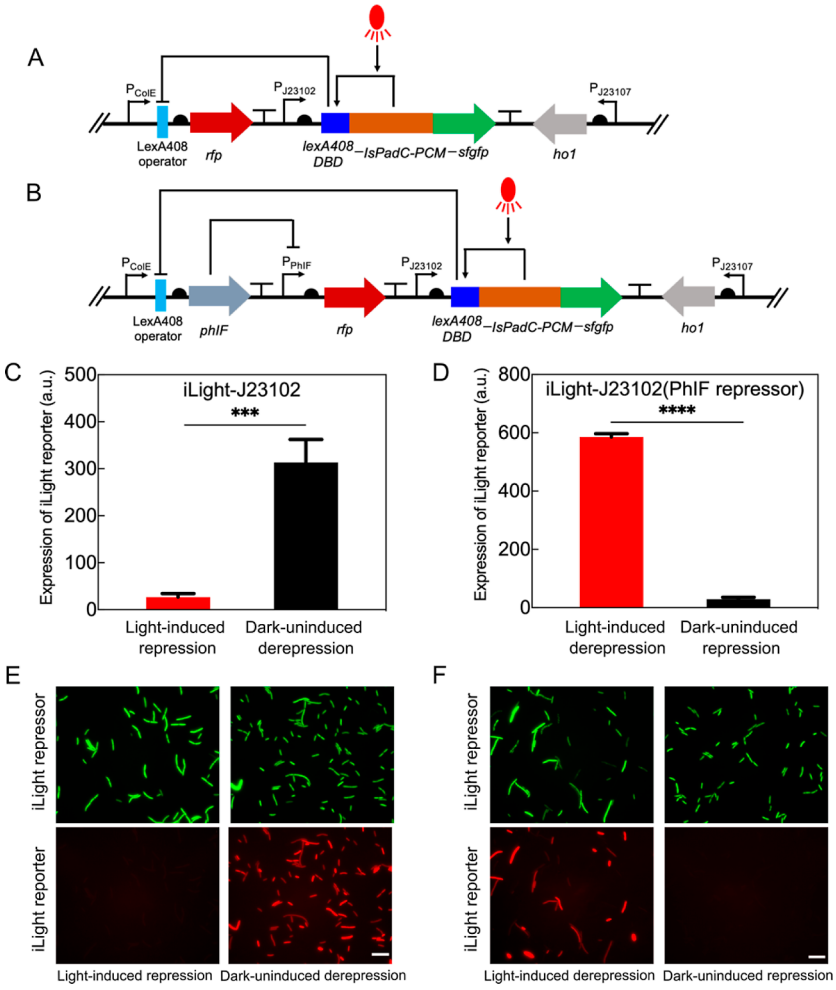

Figure 3. Characterization of the noninverted iLight genetic circuit iLight-J23102 and the inverted iLight genetic circuit iLight-J23102(PhlF repressor) in *S. oneidensis*. (A) Genetic circuit of noninverted iLight-J23102. (B) Genetic circuit of the inverted iLight-J23102(PhlF repressor). This circuit was generated by adding the gene of a second repressor PhlF and its cognate promoter to the genetic circuit iLight-J23102. The transcription of the PhlF repressor gene is controlled by the iLight repressor, while the transcription of the RFP reporter gene is repressed by the PhlF repressor. (C) RFP fluorescence intensity measurements of iLight reporter expression in the noninverted iLight-J23102 strain cultured under red light and dark conditions, respectively. $p = 0.0006$ for light vs dark (two-tailed unpaired *t*-test). (D) RFP fluorescence intensity measurements of iLight reporter expression in the inverted iLight-J23102(PhlF repressor) strain cultured under red light and dark conditions, respectively. $p < 0.0001$ for light vs dark (two-tailed unpaired *t*-test). (E) Microscopic observation of iLight reporter and iLight repressor for noninverted iLight-J23102 cells cultured under red light and dark conditions, respectively. (F) Microscopic observation of iLight reporter and iLight repressor for inverted iLight-J23102(PhlF repressor) cells cultured under red light and dark conditions, respectively. Scale bars: 10 μm. The measurements (mean ± SD) were derived from triplicate experiments. a.u., arbitrary units. Significance is indicated as ***$p < 0.001$ and ****$p < 0.0001$.

https://doi.org/10.1021/acssynbio.3c00684
ACS Synth. Biol. 2024, 13, 1467–1476

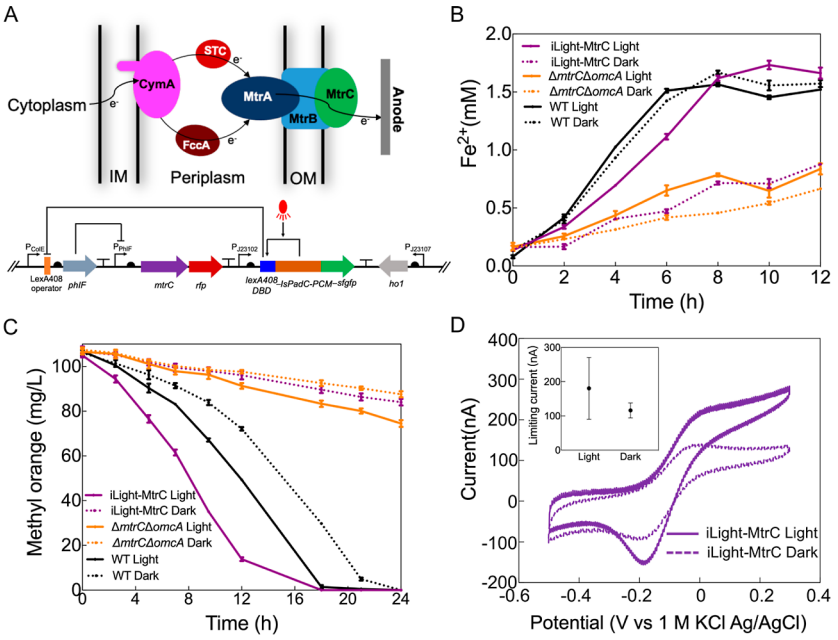

Figure 4. Using an iLight-J23102(PhIF repressor) genetic circuit to control the outer membrane cytochrome MtrC expression for light-induced EET activity in *S. oneidensis*. (A) EET pathway of *S. oneidensis* MR-1 and the genetic circuit of iLight-MtrC, which used the iLight-J23102(PhIF repressor) genetic circuit to control MtrC expression. (B) Iron reduction assay for the iLight-MtrC strain, Δ*mtrC*Δ*omcA*, and wild type with blank plasmid iLight-J23102(PhIF repressor) after being cultured under red light and dark conditions, respectively. (C) Methyl orange decoloration assay for iLight-MtrC strain, Δ*mtrC*Δ*omcA*, and wild type with blank plasmid iLight-J23102(PhIF repressor) after being cultured under red light and dark conditions, respectively. (D) CV curves for the iLight-MtrC strain after being cultured under red light and dark conditions, respectively. The inset graph shows the average limiting current from CV measurements of three biological replicates. Data show mean ± SD from triplicate experiments.

gene expression in light and dark conditions might depend on the level of repressor expression. To test this hypothesis, we first developed a thermodynamic model to predict how the expression level of the iLight repressor impacts the fold change of the iLight reporter when exposed to dark and light conditions (see Supporting Information and Figure S2). The thermodynamic model[36−38] investigates RFP gene expression considering the binding probabilities of RNA polymerase and iLight repressor molecules to the promoter region in red light and dark conditions (Figure S2A). Additionally, it assumes that the dimeric form of the iLight repressor in dark exhibits a nonzero, but lower, probability of binding to the specific site compared to the tetrameric form in red light. We found that the fold change in gene expression was largest for intermediate expression levels of iLight repressor (Figure S2B,C), suggesting that increasing expression of the iLight repressor might improve the performance of this optogenetic circuit within *S. oneidensis*.

The expression of the iLight repressor was modified by site-directed mutagenesis of the promoter region (Figure 2A). The original promoter J23116 is weak.[39] Based on the Anderson promoter collection (http://parts.igem.org/Promoters/Catalog/Anderson), the promoter of the iLight repressor was mutated to achieve a broad range of expression levels. As shown in Figure 2B, the modified promoters varied in expression of the iLight repressor over 44-fold. Expression of the RFP iLight reporter gene in both light and dark conditions was measured for each of these promoters (Figure S3). Promoters J23102 and J23108, which expressed intermediate levels of the iLight repressor, showed the largest fold change of the iLight reporter (Figure 2C). The fold changes of the iLight reporter (dark/red light) were around 12 for both iLight-J23102 and iLight-J23108 (Figure 2C). We also tested the performance of these iLight genetic circuits with modified expression of the iLight repressor in *E. coli*. The fold change in expression of the iLight reporter decreased to 1 at high levels of iLight repressor expression (Figure S4). Unlike in *S. oneidensis*, the weakest promoters resulted in fold changes above 20, likely due to these weak promoters having higher expression in *E. coli* than in *S. oneidensis*. In summary, implementation of the iLight optogenetic system for use in *S. oneidensis* required the adjustment of the expression level of the iLight repressor.

Creating an Inverted iLight Optogenetic System for Light-Activated Gene Regulation. The iLight optogenetic system could work in *S. oneidensis* MR-1 after adjusting the expression level of the iLight repressor. In the original report, the iLight system was used to repress gene expression in *E. coli* with red light (Figure 3A), but other optogenetic circuits have been modified for both activation and repression with light inputs. Next, we improved the iLight optogenetic system to activate the target gene expression through red light illumination in *S. oneidensis* MR-1.

To accomplish this, we incorporated the iLight repressor into an inverter genetic circuit by adding a second repressor. Expression of the second repressor regulates the target gene and is regulated by the iLight repressor. After red light illumination, the expression of this second repressor is repressed by the iLight repressor, resulting in derepression of the target gene (Figure 3B). We tested three different repressors, the λ phage repressor cI and the TetR-family repressors PhIF and SrpR,[40] with their cognate promoters to invert the iLight-J23102 genetic circuit. All three repressors resulted in increased expression of the target gene in response

https://doi.org/10.1021/acssynbio.3c00684
ACS Synth. Biol. 2024, 13, 1467−1476

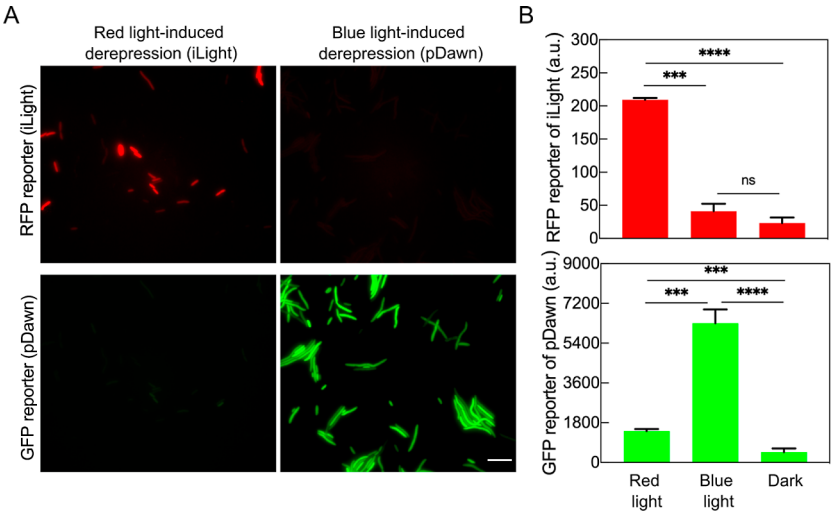

Figure 5. Introduction of two optogenetic systems, iLight and pDawn, into *S. oneidensis*. (A) Microscopic observation of RFP and GFP reporters for *S. oneidensis* cells with both iLight and pDawn genetic circuits cultured under red and blue light conditions, respectively. Scale bar 10 μm. (B) Fluorescence intensity measurements of RFP and GFP reporters in *S. oneidensis* cells with both iLight and pDawn genetic circuits cultured under red light, blue light, and dark conditions, respectively. The measurements were performed by a plate reader (Infinite 200 PRO, Tecan). Data shows mean ± SD from triplicate experiments. a.u., arbitrary units. $p = 0.0001$ for fluorescence intensity of RFP reporter under red light vs under blue light. $p < 0.0001$ for fluorescence intensity of RFP reporter under red light vs under dark. $p = 0.0633$ for fluorescence intensity of RFP reporter under blue light vs under dark. $p = 0.0002$ for fluorescence intensity of GFP reporter under blue light versus under red light. $p < 0.0001$ for fluorescence intensity of GFP reporter under blue light vs under dark. $p = 0.0001$ for fluorescence intensity of GFP reporter under red light vs under dark. Two-tailed unpaired *t*-test was used for statistical analyses. Significance is indicated as ***$p < 0.001$, ****$p < 0.0001$, and ns (not significant) $p > 0.05$.

to red light (Figures 3D and S5A−C). The fold changes of iLight reporter RFP between red light and dark conditions were 16 for cI repressor, 20 for PhIF repressor, and 12 for SrpR repressor (Figures 3D and S5A−C). Microscopic images showed that the noninverted iLight-J23102 cells had strong red fluorescence after being cultured under dark but weak fluorescence after being cultured with red light (Figure 3E), as expected for light-induced repression of gene expression. The microscopic images of the inverted iLight-J23102(PhIF repressor) strain showed that the cells had strong red fluorescence after being cultured with red light but weak fluorescence after being cultured in the dark (Figure 3F), as expected for light-induced activation of gene expression. Introduction of the iLight optogenetic system into *S. oneidensis* did not have an obvious detrimental effect on cell growth rate (Figure S6). We also found that inverting the iLight-J23108 genetic circuit using the cI repressor resulted in a 5-fold change in reporter gene expression (Figure S5D), which was much lower than that of inverting iLight-J23102 (Figure S5A). The reason for this could be higher leaky expression of the inverting repressor (cI) for iLight-J23108 relative to iLight-J23102 under red light condition (Figure S3). We selected the iLight-J23102(PhIF repressor) genetic circuit, which had the highest fold change, for subsequent experiments.

Taken collectively, we inverted the iLight optogenetic system to activate the target gene expression under red light illumination in *S. oneidensis*, and the fold change was increased compared with the noninverted iLight genetic circuit.

Extracellular Electron-Transfer Activity of *S. oneidensis* Can Be Regulated with Red Light. *S. oneidensis* MR-1 can transport electrons from cytosolic metabolism to external electrodes using an EET pathway involving *c*-type cytochromes located in the inner membrane, periplasm, and outer membrane[18] (Figure 4A). To determine if we can control the EET activity of *S. oneidensis* by using light, we used the iLight optogenetic system to control the expression of multiple cytochromes within this EET pathway. We constructed a *S. oneidensis* strain iLight-MtrC, which utilized the inverted iLight-J23102(PhIF repressor) genetic circuit to activate the expression of the outer membrane cytochrome MtrC with red light (Figure 4A). The genetic background for this strain is *S. oneidensis* Δ*mtrC*Δ*omcA*[41] in which the key genes encoding outer membrane cytochromes were deleted from the genome. MtrC expression from the promoter was evaluated by measuring the RFP fluorescence under aerobic conditions due to the RFP gene cotranscribed from the same promoter (Figure 4A). As expected, RFP fluorescence was higher when culturing the iLight-MtrC strain under red light illumination, than when cultured in the dark (Figure S7). A heme-stained protein gel showed that the iLight-MtrC strain had a band corresponding to MtrC when cultured aerobically under red light, which was comparable to the MtrC bands of wild type cultured either under red light or in the dark (Figure S8). The iLight-MtrC strain had no visible band of MtrC cytochrome when grown in the dark (Figure S8). The results collectively suggest that MtrC could be expressed under red light illumination with a very low expression in the dark.

Next, EET activity was measured for the iLight-MtrC strain cultured under light and dark conditions by using colorimetric assays for extracellular redox activity. *S. oneidensis* can perform anaerobic respiration by reducing a wide range of external terminal electron acceptors.[42−47] We utilized iron citrate and methyl orange (MO) as the electron acceptors to measure the Fe^{3+} and azo dye reduction capabilities of the iLight-MtrC strain. As shown in Figure 4B,C, the iLight-MtrC strain had much higher Fe^{3+} and MO reduction rates when cultured under red light than those of iLight-MtrC grown in the dark. The reduction activities of red-light-illuminated iLight-MtrC cells were comparable with those of wild-type cells cultured either under red light or in the dark. The reduction activities of

https://doi.org/10.1021/acssynbio.3c00684
ACS Synth. Biol. 2024, 13, 1467−1476

iLight-MtrC cells grown in the dark were as low as those of Δ*mtrC*Δ*omcA* cultured either under red light or in the dark (Figure 4B,C). Slightly higher MO reduction rates of the wild type and Δ*mtrC*Δ*omcA* were observed when cultured under red light. There is no clear explanation for this small increase in activity. The larger change in redox activity of the iLight-MtrC strain indicates that the reduction activity switches from Δ*mtrC*Δ*omcA* to wild-type levels under red light conditions.

Finally, we performed electrochemical measurements to determine whether light-induced expression of MtrC would modulate current production in *S. oneidensis* biofilms. Cells were grown in bioreactors with planar indium tin oxide (ITO)-coated glass coverslips as the bottom with or without red light illumination. Cyclic voltammetry (CV) was performed for the biofilms on the ITO electrodes. As shown in the cyclic voltammetry curves in Figure 4D, we found a higher current for the red-light-illuminated iLight-MtrC cells than for the same strain grown in the dark. The average limiting currents from cyclic voltammetry measurements of three biological replicates were 180 nA for red-light-illuminated cells and 110 nA for cells cultured under dark conditions (Figure 4D inset graph).

We also constructed a *S. oneidensis* strain iLight-STC to use the iLight-J23102(PhIF repressor) genetic circuit to control expression of the periplasmic small tetraheme cytochrome (STC, encoded by the gene *cctA*)[48] by red light within *S. oneidensis* Δ*stc*Δ*fccA*. STC could be expressed under red light illumination with very low expression in the dark (Figure S9A). The Fe^{3+} reduction activities of the iLight-STC strain could also be controlled by red light (Figure S9B). These results demonstrate that we can regulate the EET activity of *S. oneidensis* using optogenetic circuits that regulate the expression of cytochrome in different cellular locations.

Introduction of Two Optogenetic Systems, iLight and pDawn, into *S. oneidensis*. We then checked if *S. oneidensis* could simultaneously utilize two different light-regulated genetic constructs to respond to different wavelengths of light. To achieve this, we introduced the blue-light-induced pDawn[3] genetic circuit to control GFP expression and the red-light-induced iLight genetic circuit to control RFP expression within *S. oneidensis*. The iLight circuit used here did not have sfGFP fusion to the iLight repressor. We also changed the antibiotic resistance of iLight genetic circuit from spectinomycin to kanamycin to make pDawn and iLight genetic circuits compatible (Tables S1 and S2). As we expected, *S. oneidensis* cells containing both iLight and pDawn genetic circuits had strong red fluorescence when cultured under red light illumination and strong green fluorescence when cultured under blue light illumination (Figure 5A,B). A small amount of expression of the RFP and GFP were triggered by blue light and red light, respectively, although there was no significant difference of RFP between blue light and dark (Figure 5B). Expressions of both RFP and GFP under the dark conditions were very weak (Figure 5B). Expressions of RFP and GFP under red light and blue light were reduced in the dual light sensor system compared to that in the single light sensor (Figure S10). Overall, these results indicated that the inverted iLight genetic circuit could work together with the blue-light-induced pDawn genetic circuit to control the expression of two different genes with two different colors of light.

DISCUSSION

We developed and adapted a red-light-induced genetic circuit for *S. oneidensis* MR-1 based on a previously reported iLight optogenetic system.[35] Through modeling and experimental tests, we found that the iLight genetic circuits required an intermediate level of the light-responsive repressor to function properly for light-regulated gene expression. Low expression of the iLight repressor resulted in insufficient formation and binding of the repressor tetramer under the red light condition, which led to insufficient repression of the iLight reporter. High expression of the iLight repressor resulted in repression of the regulated gene under both dark and light conditions, as the large concentration of the repressor compensated for the weak binding of the repressor in the dark state. This work demonstrated how the expression levels of transcription factor proteins can be critical to the function of a genetic circuit, and a similar promoter optimization may be needed to adapt the iLight optogenetic system in other bacterial host strains.

To expand the regulatory capability of the iLight system in *S. oneidensis*, we inverted the iLight genetic circuit by adding an additional repressor to activate the gene expression by red light (Figure 3). We selected three different repressors with their cognate promoters.[40] Inverting iLight with cI and PhIF repressors achieved a higher expression of RFP than with a circuit using the SrpR repressor. The fold changes in gene expression were greater in the inverted iLight genetic circuit containing cI and PhIF repressors than in the noninverted iLight. The reason could be that the cognate promoters of cI and PhIF repressors are stronger than the ColE promoter, so expression levels of RFP are higher in inverted iLight under red light than that of noninverted iLight under dark. A similar trend was observed for the blue-light-induced pDawn and pDusk genetic circuits.[3]

Prior efforts to regulate the EET activity of *S. oneidensis* usually depended on using chemically induced genetic circuits to control the expression of cytochromes.[25,27,28] Compared with chemically induced genetic circuits, light-induced genetic circuits make it possible to create spatial patterns of microbial activity.[9,10,12,13] Our work using the red-light-induced iLight genetic circuit to control cytochrome expression further expands the synthetic biology toolboxes of *S. oneidensis* and demonstrates light-induced EET activities, which can be a promising approach to spatiotemporally control the EET of *S. oneidensis*. We also indicated the potential of using two optogenetic systems, iLight and pDawn, to simultaneously regulate expression of two different genes in *S. oneidensis*, although there was upregulated expression of both genes by the other color of light (Figure 5). Combined with our previous blue-light-induced conductive biofilm patterning technique, the dual-light control system can be promising to control the electron transfer of *S. oneidensis* at different scales. The programmable control of electron transfer in *S. oneidensis* using light will have implications for studying and developing living electronics, which can be used for biosensing,[49] biosynthesis,[50,51] electroactive biomaterials,[34,52] and biocomputing.[53,54]

METHODS

Bacterial Strains and Plasmids. *E. coli* DH5α and NEB-stable were used for plasmid construction. *S. oneidensis* MR-1 was used as the host to characterize the performances of different noninverted and inverted iLight constructs in *S.*

https://doi.org/10.1021/acssynbio.3c00684
ACS Synth. Biol. 2024, 13, 1467−1476

oneidensis. *S. oneidensis* Δ*mtrC*Δ*omcA* (strain JG749)[41] was used as the host to contain the plasmid with expression of outer membrane cytochrome MtrC controlled by the inverted iLight genetic circuit. *S. oneidensis* Δ*stc*Δ*fccA* (strain JG3107) was used as the host to contain the plasmid, with expression of periplasm cytochrome STC controlled by the inverted iLight genetic circuit. The Δ*stc*Δ*fccA* strain was generated by deleting *fccA* using materials and methods described previously[55] in strain JG561, a background where *cctA* has been deleted.[41] *E. coli* NEB-stable was used as the host to characterize the performances of different noninverted iLight constructs in *E. coli*.

The original iLight plasmid[35] was purchased from Addgene (catalog no. 170268). A *ho1* gene was amplified from plasmid pNO41[5] (Addgene, catalog no. 101067) and then added to the original iLight plasmid to create the iLight-J23116 plasmid. To construct iLight plasmids with different promoters expressing the iLight repressor, iLight-J23116 was used as the starting plasmid. Site-directed mutagenesis was then performed for the promoter region of iLight repressor through using an NEB Q5 Site-Directed Mutagenesis Kit with nonoverlapping primers or NEBuilder HiFi DNA Assembly (New England BioLabs, MA, USA) with overlapping primers. cI, PhIF, and SrpR repressors with their cognate promoters were amplified from plasmid pDawn-mCherry,[34] pRF-PhIF[40] (Addgene, catalog no. 49367), and pRF-SrpR[40] (Addgene, catalog no. 49372), respectively. Then, these DNA fragments were added to the iLight-J23102 and iLight-J23108 plasmids after the LexA408 operator to obtain different inverted iLight genetic circuits. To test whether *S. oneidensis* could utilize iLight and pDawn genetic circuits to respond to red and blue light simultaneously, we constructed a plasmid to control GFP expression by pDawn. We removed the GFP reporter for the expression of the iLight repressor and changed the antibiotic resistance from spectinomycin to kanamycin in the iLight plasmid. For constructing light-induced EET plasmids, the *mtrC* and *stc* genes were amplified from the genome of *S. oneidensis* MR-1 and added before the *mCherry* gene in the inverted iLight plasmids under the control of the cognate promoter of the second repressor.

All strains, plasmids, and primers used in this study are listed in Tables S1−S3.

Growth Conditions. *E. coli* strains were cultivated in lysogeny broth (LB) medium (10 g/L tryptone, 5 g/L yeast extract, and 5 g/L sodium chloride) at 37 °C and 200 rpm with an orbital throw of 2.5 cm. *S. oneidensis* strains were cultivated in LB medium or minimal medium at 30 °C and 200 rpm with an orbital throw of 2.5 cm. The minimal medium recipe can be found in Table S4. When necessary, media were supplemented with spectinomycin (Spec, 100 μg/mL) and kanamycin (Kan, 50 μg/mL). To obtain growth curves of different *S. oneidensis* strains, optical density measurements (OD_{600nm}) were made at fixed time intervals using a spectrophotometer (Spectronic 200, Thermo Scientific).

For the anaerobic culturing of *S. oneidensis*, the minimal media with either iron citrate or methyl orange as electron acceptors were purged with nitrogen. For electrochemical measurements, minimal medium without vitamin solution was purged with nitrogen. Anaerobic culturing was performed in sealed serum bottles and electrochemical measurements were performed in an anaerobic chamber.

Fluorescence Measurements and Microscopy. To characterize performance of the iLight genetic circuits in *E. coli* and *S. oneidensis*, overnight cultures (1%, v/v) started from frozen stocks of the strains were transferred into 5 mL of fresh LB broth and grown to the log phase (OD_{600nm} about 1−1.5). Then, the cultures (1%, v/v) were seeded into 5 mL of LB broth and incubated at 37 or 30 °C, for *E. coli* and *S. oneidensis*, respectively, either under red light or dark conditions while shaking at 200 rpm with an orbital throw of 2.5 cm. Red light was provided by attaching LED strip lights (Deep Cool RGB 350) to the wall inside the shaker with an intensity of 150 μW/cm.[2,35] *S. oneidensis* containing both the pDawn and iLight genetic circuits were exposed to blue light and red light, both with intensities of 150 $\mu W/cm^2$. Media were supplemented with kanamycin (50 μg/mL) to select the iLight plasmids and spectinomycin (100 μg/mL) to select the pDawn plasmids. An optical power meter (PM100USB, Thorlabs) was used for measuring the illumination intensity of the lights. Cultures were collected after 18 h incubation to measure the fluorescence of RFP and GFP, and the cell optical density (OD_{600nm}). High-magnification fluorescence images showed a uniform fluorescence response from the cells, suggesting stable inheritance of the plasmid during the laboratory culture. Quantitative RFP and GFP fluorescence measurements were performed via a plate reader (Infinite 200 PRO, Tecan) at an excitation wavelength of 590 nm and an emission wavelength of 650 nm for RFP and an excitation wavelength of 485 nm and an emission wavelength of 515 nm for GFP. The OD_{600nm} was determined using a spectrophotometer (Spectronic 200, Thermo Scientific). Relative fluorescence intensity was calculated by normalization against the OD_{600nm} of whole cells. Autofluorescence was subtracted by measuring the fluorescence of wild-type strains. Fluorescence of RFP and GFP was imaged via a fluorescent microscope equipped with a 100× oil immersion objective lens (Revolve, Echo).

Iron Reduction Measurements. Resting cell ferrozine assay[25] was used to measure the Fe^{3+} reduction abilities of *S. oneidensis* strains. Cells from log phase LB cultures were diluted into 5 mL of fresh LB broth. Then, cells were incubated for 18 h at 30 °C under either red light or dark conditions while shaking at 200 rpm with an orbital throw of 2.5 cm. Cells were collected by centrifuging (5840R, Eppendorf) at 4200 rpm, 4 °C for 15 min and then washed with fresh minimal medium 2 times. After that, cells were inoculated into sealed serum bottles containing 25 mL of anaerobic minimal medium to an OD_{600nm} of about 0.1. 2 mM ferric citrate was added into the anaerobic minimal medium as the electron acceptor. The samples were incubated at 30 °C in the dark without shaking. Every 2 h, 10 μL of each sample was added immediately to 90 μL of 1 M HCl in a 96-well plate followed by 100 μL of 0.01% ferrozine. Then, after the samples were mixed well and allowed to sit for 10 min, the absorbance of the samples at 562 nm was determined with a plate reader (Infinite 200 PRO, Tecan). A standard curve of freshly made ferrous sulfate was used to determine the Fe^{2+} concentrations.

MO Reduction Measurements. The MO decoloration assay[47] was used to measure the MO reduction abilities of *S. oneidensis* strains. The preculture was the same as the iron reduction measurements. Cells after being cultured under either red light or dark condition were washed and inoculated into sealed serum bottles containing 25 mL of anaerobic minimal medium with 100 mg/L MO as the electron acceptor to an OD_{600nm} of about 0.1. The samples were cultured at 30 °C, 200 rpm with an orbital throw of 2.5 cm under either red light or dark condition. Absorbances of the samples from

https://doi.org/10.1021/acssynbio.3c00684
ACS Synth. Biol. 2024, 13, 1467−1476

different culturing times were measured at 465 nm with a plate reader (Infinite 200 PRO, Tecan). A standard curve of absorbances of freshly made MO with different concentrations was used to determine the MO concentrations of the samples.

Transparent-Bottom Bioreactor Construction. Bioreactor construction was performed as in our previous work.[34] In brief, planar commercial ITO-coated glass coverslips (22 mm × 40 mm) were used as the working electrodes (WEs) and the base of the bioreactors. Thin copper wires were electrically connected to the WEs with silver paint, and the wire-electrode connections were then strengthened by covering with epoxy. Glass tubes (2.5 cm tall with 20 and 22 mm inner and outer diameters, respectively) were adhered overtop of the WEs with siliconized sealant as the body of the bioreactors. Custom, PEEK plastic lids were used with the bioreactors along with custom Pt wire counter electrodes (CEs) and 1 M KCl Ag/AgCl reference electrodes (REs). During cell culturing within the bioreactors, the PEEK plastic lids along with CEs and REs were removed from the bioreactors, and the bioreactors were simply used as culturing vessels.

Cell Culturing and Biofilm Formation within Bioreactors. Cell culturing within the bioreactor was modified based on our previous work.[34] Log phase LB cultures (OD_{600nm} about 1−1.5) were diluted into fresh minimal medium to an OD_{600nm} of about 0.01. 1 mL of the diluted culture was added to the bioreactor, which was made by attaching a 20 mm diameter and 2.5 cm tall glass tube on an ITO-coated glass coverslip. The glass tube was sealed with a microporous membrane filter and taped to the ceiling of an incubator. A portable smart projector (A5 Pro, Wowoto) was secured below the bioreactor in the incubator and pointed up at the bottom surface of the bioreactor to shine red light with an intensity of 150 $\mu W/cm^2$. The dark samples were covered with aluminum foil to prevent undesired photoactivation. After 18 h of culturing at 30 °C in the incubator under either red light or dark condition, the medium was discarded, and the biofilms on the ITO electrodes were washed 3 times, for 2 min each time, with minimal medium on a table shaker at 60 rpm to remove the planktonic cells. The bioreactors with fresh minimal medium were then moved to the anaerobic chamber for electrochemical measurements.

Electrochemical Activity Measurements. All electrochemical measurements were performed in an anaerobic chamber (Bactron 300, Sheldon Manufacturing, Inc.) under a 95:5 (N_2/H_2) atmosphere. Electrochemical measurements were performed with sterile minimal medium as a blank before the bioreactors were used for cell culturing. After culturing and washing the biofilms, the reactor media were exchanged for anoxic media inside the anaerobic chamber before all electrochemical measurements. Biofilm CV measurements were performed from −500 to 300 mV at 1 mV/s using a four-channel Squidstat (Admiral Instruments). Three cycles were performed for the CV, and data from only the third cycle was presented in this article. All potentials reported in this article are vs 1 M KCl Ag/AgCl.

Statistical Analysis. All statistical analyses were performed by the Prism software (version 9.0; GraphPad) using the two-tailed unpaired *t*-test. All data are presented as the mean ± SD. *p* values in all graphs were generated with tests as indicated in figure legends and are represented as follows: $*p < 0.05$, $**p < 0.01$, $***p < 0.001$, $****p < 0.0001$, and ns (not significant) $p > 0.05$.

■ ASSOCIATED CONTENT

Data Availability Statement

All relevant data supporting the key findings of this study are available within the article and Supporting Information. Plasmids and strains generated for this study will be shared upon request to the corresponding author.

Supporting Information

The Supporting Information is available free of charge at https://pubs.acs.org/doi/10.1021/acssynbio.3c00684.

Plasmids, strains, and primers used in this study; recipe of *S. oneidensis* MR-1 minimal medium; characterization of the iLight optogenetic system without containing the heme oxygenase gene *ho1*; thermodynamic model of the iLight optogenetic system; expression of the iLight reporter in *S. oneidensis* strains containing different promoters of iLight repressor; characterization of the iLight genetic circuits with different promoters of iLight repressor in *E. coli*; characterization of the inverted iLight genetic circuits in *S. oneidensis*; growth curves of *S. oneidensis* strains cultured aerobically in LB medium; expression of outer membrane cytochrome MtrC through inverted iLight genetic circuit in *S. oneidensis*; TMBZ heme stained protein gel of light-induced expression of cytochrome MtrC; expression of periplasm cytochrome STC through inverted iLight genetic circuit in *S. oneidensis*; and comparison of RFP and GFP expression under red light and blue light between the dual light sensor system and single light sensor system (PDF)

■ AUTHOR INFORMATION

Corresponding Author

James Q. Boedicker − *Department of Physics and Astronomy, University of Southern California, Los Angeles, California 90089, United States; Department of Biological Sciences, University of Southern California, Los Angeles, California 90089, United States;* orcid.org/0000-0003-4107-3719; Email: boedicke@usc.edu

Authors

Fengjie Zhao − *Department of Physics and Astronomy, University of Southern California, Los Angeles, California 90089, United States;* orcid.org/0000-0003-2279-5062

Christina M. Niman − *Department of Physics and Astronomy, University of Southern California, Los Angeles, California 90089, United States*

Ghazaleh Ostovar − *Department of Physics and Astronomy, University of Southern California, Los Angeles, California 90089, United States*

Marko S. Chavez − *Department of Physics and Astronomy, University of Southern California, Los Angeles, California 90089, United States;* orcid.org/0009-0005-3846-9749

Joshua T. Atkinson − *Department of Physics and Astronomy, University of Southern California, Los Angeles, California 90089, United States; Department of Civil and Environmental Engineering and Omenn-Darling Bioengineering Institute, Princeton University, Princeton, New Jersey 08540, United States*

Benjamin M. Bonis − *BioTechnology Institute and Department of Plant and Microbial Biology, University of Minnesota—Twin Cities, St. Paul, Minnesota 55108, United States*

Jeffrey A. Gralnick − *BioTechnology Institute and Department of Plant and Microbial Biology, University of Minnesota—Twin Cities, St. Paul, Minnesota 55108, United States;* orcid.org/0000-0001-9250-7770

Mohamed Y. El-Naggar − *Department of Physics and Astronomy, University of Southern California, Los Angeles, California 90089, United States; Department of Biological Sciences and Department of Chemistry, University of Southern California, Los Angeles, California 90089, United States;* orcid.org/0000-0001-5599-6309

Complete contact information is available at: https://pubs.acs.org/10.1021/acssynbio.3c00684

Author Contributions

F.Z., J.T.A., J.A.G., M.Y.E.-N., and J.Q.B. designed research; F.Z. performed most of the research; C.M.N. and M.S.C. helped perform the electrochemical measurements; G.O. helped create the model; B.M.B. generated a strain used in this work; F.Z., C.M.N., G.O., and J.Q.B. analyzed the data; and F.Z., G.O., and J.Q.B. wrote the paper. All authors edited the manuscript.

Notes

The authors declare no competing financial interest.

■ ACKNOWLEDGMENTS

This study was supported by the US Office of Naval Research Multidisciplinary University Research Initiative grant no. N00014-18-1-2632. J.Q.B. acknowledges support from the Army Research Office under cooperative agreement number W911NF-24-2-0003. J.T.A. was supported by the NSF Postdoctoral Research Fellowships in Biology Program under grant no. 2010604.

■ REFERENCES

(1) Lindner, F.; Diepold, A. Optogenetics in Bacteria—Applications and Opportunities. *FEMS Microbiol. Rev.* **2022**, *46*, fuab055.

(2) Levskaya, A.; Chevalier, A. A.; Tabor, J. J.; Simpson, Z. B.; Lavery, L. A.; Levy, M.; Davidson, E. A.; Scouras, A.; Ellington, A. D.; Marcotte, E. M.; Voigt, C. A. Engineering *Escherichia coli* to See Light. *Nature* **2005**, *438*, 441−442.

(3) Ohlendorf, R.; Vidavski, R. R.; Eldar, A.; Moffat, K.; Möglich, A. From Dusk till Dawn: One-Plasmid Systems for Light-Regulated Gene Expression. *J. Mol. Biol.* **2012**, *416* (4), 534−542.

(4) Tabor, J. J.; Levskaya, A.; Voigt, C. A. Multichromatic Control of Gene Expression in *Escherichia coli*. *J. Mol. Biol.* **2011**, *405* (2), 315−324.

(5) Ong, N. T.; Olson, E. J.; Tabor, J. Engineering an *E. coli* Near-Infrared Light Sensor. *ACS Synth. Biol.* **2018**, *7*, 240−248.

(6) Fernandez-Rodriguez, J.; Moser, F.; Song, M.; Voigt, C. A. Engineering RGB Color Vision into *Escherichia coli*. *Nat. Chem. Biol.* **2017**, *13* (7), 706−708.

(7) Multamäki, E.; García de Fuentes, A.; Sieryi, O.; Bykov, A.; Gerken, U.; Ranzani, A. T.; Köhler, J.; Meglinski, I.; Möglich, A.; Takala, H. Optogenetic Control of Bacterial Expression by Red Light. *ACS Synth. Biol.* **2022**, *11*, 3354−3367.

(8) Zhao, E. M.; Zhang, Y.; Mehl, J.; Park, H.; Lalwani, M. A.; Toettcher, J. E.; Avalos, J. L. Optogenetic Regulation of Engineered Cellular Metabolism for Microbial Chemical Production. *Nature* **2018**, *555*, 683−687.

(9) Lalwani, M. A.; Ip, S. S.; Carrasco-López, C.; Day, C.; Zhao, E. M.; Kawabe, H.; Avalos, J. L. Optogenetic Control of the Lac Operon for Bacterial Chemical and Protein Production. *Nat. Chem. Biol.* **2021**, *17*, 71−79.

(10) Tandar, S. T.; Senoo, S.; Toya, Y.; Shimizu, H. Optogenetic Switch for Controlling the Central Metabolic Flux of *Escherichia coli*. *Metab. Eng.* **2019**, *55*, 68−75.

(11) Wu, P.; Chen, Y.; Liu, M.; Xiao, G.; Yuan, J. Engineering an Optogenetic CRISPRi Platform for Improved Chemical Production. *ACS Synth. Biol.* **2021**, *10*, 125−131.

(12) Jin, X.; Riedel-Kruse, I. H. Biofilm Lithography Enables High-Resolution Cell Patterning via Optogenetic Adhesin Expression. *Proc. Natl. Acad. Sci. U.S.A.* **2018**, *115* (14), 3698−3703.

(13) Moser, F.; Tham, E.; González, L. M.; Lu, T. K.; Voigt, C. A. Light-Controlled, High-Resolution Patterning of Living Engineered Bacteria Onto Textiles, Ceramics, and Plastic. *Adv. Funct. Mater.* **2019**, *29* (30), 1901788.

(14) Cheng, X.; Pu, L.; Fu, S.; Xia, A.; Huang, S.; Ni, L.; Xing, X.; Yang, S.; Jin, F. Engineering Gac/Rsm Signaling Cascade for Optogenetic Induction of the Pathogenicity Switch in *Pseudomonas aeruginosa*. *ACS Synth. Biol.* **2021**, *10*, 1520−1530.

(15) Castillo-hair, S. M.; Baerman, E. A.; Fujita, M.; Igoshin, O. A.; Tabor, J. J. Optogenetic Control of *Bacillus subtilis* Gene Expression. *Nat. Commun.* **2019**, *10*, 3099.

(16) Pu, L.; Yang, S.; Xia, A.; Jin, F. Optogenetics Manipulation Enables Prevention of Biofilm Formation of Engineered *Pseudomonas aeruginosa* on Surfaces. *ACS Synth. Biol.* **2018**, *7* (1), 200−208.

(17) Myers, C. R.; Nealson, K. H. Bacterial Manganese Reduction and Growth with Manganese Oxide as The Sole Electron Acceptor. *Science* **1988**, *240*, 1319−1321.

(18) Shi, L.; Dong, H.; Reguera, G.; Beyenal, H.; Lu, A.; Liu, J.; Yu, H. Q.; Fredrickson, J. K. Extracellular Electron Transfer Mechanisms between Microorganisms and Minerals. *Nat. Rev. Microbiol.* **2016**, *14* (10), 651−662.

(19) McMillan, D. G. G.; Marritt, S. J.; Butt, J. N.; Jeuken, L. J. C. Menaquinone-7 Is Specific Cofactor in Tetraheme Quinol Dehydrogenase CymA. *J. Biol. Chem.* **2012**, *287* (17), 14215−14225.

(20) Edwards, M. J.; White, G. F.; Butt, J. N.; Richardson, D. J.; Clarke, T. A. The Crystal Structure of a Biological Insulated Transmembrane Molecular Wire. *Cell* **2020**, *181* (3), 665−673.e10.

(21) Fonseca, B. M.; Paquete, C. M.; Neto, S. E.; Pacheco, I.; Soares, C. M.; Louro, R. O. Mind the Gap: Cytochrome Interactions Reveal Electron Pathways across the Periplasm of *Shewanella oneidensis* MR-1. *Biochem. J.* **2013**, *449* (1), 101−108.

(22) Edwards, M. J.; White, G. F.; Lockwood, C. W.; Lawes, M. C.; Martel, A.; Harris, G.; Scott, D. J.; Richardson, D. J.; Butt, J. N.; Clarke, T. A. Structural Modeling of an Outer Membrane Electron Conduit from a Metal-Reducing Bacterium Suggests Electron Transfer via Periplasmic Redox Partners. *J. Biol. Chem.* **2018**, *293* (21), 8103−8112.

(23) Hartshorne, R. S.; Reardon, C. L.; Ross, D.; Nuester, J.; Clarke, T. A.; Gates, A. J.; Mills, P. C.; Fredrickson, J. K.; Zachara, J. M.; Shi, L.; Beliaev, A. S.; Marshall, M. J.; Tien, M.; Brantley, S.; Butt, J. N.; Richardson, D. J. Characterization of an Electron Conduit between Bacteria and the Extracellular Environment. *Proc. Natl. Acad. Sci. U.S.A.* **2009**, *106* (52), 22169−22174.

(24) White, G. F.; Shi, Z.; Shi, L.; Wang, Z.; Dohnalkova, A. C.; Marshall, M. J.; Fredrickson, J. K.; Zachara, J. M.; Butt, J. N.; Richardson, D. J.; Clarke, T. A. Rapid Electron Exchange between Surface-Exposed Bacterial Cytochromes and Fe(III) Minerals. *Proc. Natl. Acad. Sci. U.S.A.* **2013**, *110* (16), 6346−6351.

(25) West, E. A.; Jain, A.; Gralnick, J. A. Engineering a Native Inducible Expression System in *Shewanella oneidensis* to Control Extracellular Electron Transfer. *ACS Synth. Biol.* **2017**, *6* (9), 1627−1634.

(26) Cao, Y.; Li, X.; Li, F.; Song, H. CRISPRi-SRNA: Transcriptional-Translational Regulation of Extracellular Electron Transfer in *Shewanella oneidensis*. *ACS Synth. Biol.* **2017**, *6* (9), 1679−1690.

(27) Dundas, C. M.; Walker, D. J. F.; Keitz, B. K. Tuning Extracellular Electron Transfer by *Shewanella oneidensis* Using Transcriptional Logic Gates. *ACS Synth. Biol.* **2020**, *9* (9), 2301−2315.

(28) Cao, Y.; Song, M.; Li, F.; Li, C.; Lin, X.; Chen, Y.; Chen, Y.; Xu, J.; Ding, Q.; Song, H. A Synthetic Plasmid Toolkit for *Shewanella oneidensis* MR-1. *Front. Microbiol.* **2019**, *10*, 410.
(29) Jensen, H. M.; Albers, A. E.; Malley, K. R.; Londer, Y. Y.; Cohen, B. E.; Helms, B. A.; Weigele, P.; Groves, J. T.; Ajo-Franklin, C. M. Engineering of a Synthetic Electron Conduit in Living Cells. *Proc. Natl. Acad. Sci. U.S.A.* **2010**, *107* (45), 19213−19218.
(30) Jensen, H. M.; TerAvest, M. A.; Kokish, M. G.; Ajo-Franklin, C. M. CymA and Exogenous Flavins Improve Extracellular Electron Transfer and Couple It to Cell Growth in Mtr-Expressing *Escherichia coli*. *ACS Synth. Biol.* **2016**, *5* (7), 679−688.
(31) Zacharoff, L. A.; El-Naggar, M. Y. Redox Conduction in Biofilms: From Respiration to Living Electronics. *Curr. Opin. Electrochem.* **2017**, *4* (1), 182−189.
(32) Atkinson, J. T.; Chavez, M. S.; Niman, C. M.; El-Naggar, M. Y. Living Electronics: A Catalogue of Engineered Living Electronic Components. *Microb. Biotechnol.* **2023**, *16* (3), 507−533.
(33) Xu, S.; Barrozo, A.; Tender, L. M.; Krylov, A. I.; El-Naggar, M. Y. Multiheme Cytochrome Mediated Redox Conduction through *Shewanella oneidensis* MR-1 Cells. *J. Am. Chem. Soc.* **2018**, *140* (32), 10085−10089.
(34) Zhao, F.; Chavez, M. S.; Naughton, K. L.; Niman, C. M.; Atkinson, J. T.; Gralnick, J. A.; El-Naggar, M. Y.; Boedicker, J. Q. Light-Induced Patterning of Electroactive Bacterial Biofilms. *ACS Synth. Biol.* **2022**, *11* (7), 2327−2338.
(35) Kaberniuk, A. A.; Baloban, M.; Monakhov, M. V.; Shcherbakova, D. M.; Verkhusha, V. V. Single-Component near-Infrared Optogenetic Systems for Gene Transcription Regulation. *Nat. Commun.* **2021**, *12* (1), 3859.
(36) Kreamer, N. N.; Phillips, R.; Newman, D. K.; Boedicker, J. Q. Predicting the Impact of Promoter Variability on Regulatory Outputs. *Sci. Rep.* **2016**, *5*, 18238.
(37) Berg, O. G.; von Hippel, P. H. Selection of DNA Binding Sites by Regulatory Proteins: Statistical-mechanical Theory and Application to Operators and Promoters. *J. Mol. Biol.* **1987**, *193*, 723−743.
(38) Guharajan, S.; Chhabra, S.; Parisutham, V.; Brewster, R. C. Quantifying the Regulatory Role of Individual Transcription Factors in *Escherichia coli*. *Cell Rep.* **2021**, *37*, 109952.
(39) Kelly, J. R.; Rubin, A. J.; Davis, J. H.; Ajo-Franklin, C. M.; Cumbers, J.; Czar, M. J.; de Mora, K.; Glieberman, A. L.; Monie, D. D.; Endy, D. Measuring the Activity of BioBrick Promoters Using an In Vivo Reference Standard. *J. Biol. Eng.* **2009**, *3*, 4.
(40) Stanton, B. C.; Nielsen, A. A. K.; Tamsir, A.; Clancy, K.; Peterson, T.; Voigt, C. A. Genomic Mining of Prokaryotic Repressors for Orthogonal Logic Gates. *Nat. Chem. Biol.* **2014**, *10* (2), 99−105.
(41) Coursolle, D.; Gralnick, J. A. Modularity of the Mtr Respiratory Pathway of *Shewanella oneidensis* Strain MR-1. *Mol. Microbiol.* **2010**, *77* (4), 995−1008.
(42) Heidelberg, J. F.; Paulsen, I. T.; Nelson, K. E.; Gaidos, E. J.; Nelson, W. C.; Read, T. D.; Eisen, J. A.; Seshadri, R.; Ward, N.; Methe, B.; Clayton, R. A.; Meyer, T.; Tsapin, A.; Scott, J.; Beanan, M.; Brinkac, L.; Daugherty, S.; DeBoy, R. T.; Dodson, R. J.; Durkin, A. S.; Haft, D. H.; Kolonay, J. F.; Madupu, R.; Peterson, J. D.; Umayam, L. A.; White, O.; Wolf, A. M.; Vamathevan, J.; Weidman, J.; Impraim, M.; Lee, K.; Berry, K.; Lee, C.; Mueller, J.; Khouri, H.; Gill, J.; Utterback, T. R.; McDonald, L. A.; Feldblyum, T. V.; Smith, H. O.; Venter, J. C.; Nealson, K. H.; Fraser, C. M. Genome Sequence of the Dissimilatory Metal Ion-Reducing Bacterium *Shewanella oneidensis*. *Nat. Biotechnol.* **2002**, *20* (11), 1118−1123.
(43) Burns, J. L.; Ginn, B. R.; Bates, D. J.; Dublin, S. N.; Taylor, J. V.; Apkarian, R. P.; Amaro-Garcia, S.; Neal, A. L.; Dichristina, T. J. Outer Membrane-Associated Serine Protease Involved in Adhesion of *Shewanella oneidensis* to Fe(III) Oxides. *Environ. Sci. Technol.* **2010**, *44* (1), 68−73.
(44) Gralnick, J. A.; Vali, H.; Lies, D. P.; Newman, D. K. Extracellular Respiration of Dimethyl Sulfoxide by *Shewanella oneidensis* Strain MR-1. *Proc. Natl. Acad. Sci. U.S.A.* **2006**, *103* (12), 4669−4674.
(45) Luan, F.; Burgos, W. D.; Xi E, L.; Zhou, Q. Bioreduction of Nitrobenzene, Natural Organic Matter, and Hematite by *Shewanella putrefaciens* CN32. *Environ. Sci. Technol.* **2010**, *44* (1), 184−190.
(46) Burns, J. L.; DiChristina, T. J. Anaerobic Respiration of Elemental Sulfur and Thiosulfate by *Shewanella oneidensis* MR-1 Requires PsrA, a Homolog of the PhsA Gene of *Salmonella enterica* Serovar Typhimurium LT2. *Appl. Environ. Microbiol.* **2009**, *75* (16), 5209−5217.
(47) Cai, P. J.; Xiao, X.; He, Y. R.; Li, W. W.; Chu, J.; Wu, C.; He, M. X.; Zhang, Z.; Sheng, G. P.; Lam, M. H. W.; Xu, F.; Yu, H. Q. Anaerobic Biodecolorization Mechanism of Methyl Orange by *Shewanella oneidensis* MR-1. *Appl. Microbiol. Biotechnol.* **2012**, *93* (4), 1769−1776.
(48) Qian, Y.; Paquete, C. M.; Louro, R. O.; Ross, D. E.; Labelle, E.; Bond, D. R.; Tien, M. Mapping the Iron Binding Site(s) on the Small Tetraheme Cytochrome of *Shewanella oneidensis* MR-1. *Biochemistry* **2011**, *50*, 6217−6224.
(49) Atkinson, J. T.; Su, L.; Zhang, X.; Bennett, G. N.; Silberg, J. J.; Ajo-Franklin, C. M. Real-Time Bioelectronic Sensing of Environmental Contaminants. *Nature* **2022**, *611*, 548−553.
(50) Fan, G.; Dundas, C. M.; Graham, A. J.; Lynd, N. A.; Keitz, B. K. *Shewanella oneidensis* As a Living Electrode for Controlled Radical Polymerization. *Proc. Natl. Acad. Sci. U.S.A.* **2018**, *115* (18), 4559−4564.
(51) Chellamuthu, P.; Naughton, K. L.; Pirbadian, S.; Silva, K. P. T.; Chavez, M.; El-Naggar, M. Y.; Boedicker, J. Q. Biogenic Control of Manganese Doping in Zinc Sulfide Nanomaterial Using *Shewanella oneidensis* MR-1. *Front. Microbiol.* **2019**, *10*, 938.
(52) Tseng, C. P.; Liu, F.; Zhang, X.; Huang, P. C.; Campbell, I.; Li, Y.; Atkinson, J. T.; Terlier, T.; Ajo-Franklin, C. M.; Silberg, J. J.; Verduzco, R. Solution-Deposited and Patternable Conductive Polymer Thin-Film Electrodes for Microbial Bioelectronics. *Adv. Mater.* **2022**, *34*, 2109442.
(53) Yim, S. S.; McBee, R. M.; Song, A. M.; Huang, Y.; Sheth, R. U.; Wang, H. H. Robust Direct Digital-to-Biological Data Storage in Living Cells. *Nat. Chem. Biol.* **2021**, *17*, 246−253.
(54) Zhang, Y.; Hsu, L. H. H.; Jiang, X. Living Electronics. *Nano Res.* **2020**, *13*, 1205−1213.
(55) Ross, D. E.; Flynn, J. M.; Baron, D. B.; Gralnick, J. A.; Bond, D. R. Towards Electrosynthesis in *Shewanella*: Energetics of Reversing the Mtr Pathway for Reductive Metabolism. *PLoS One* **2011**, *6* (2), No. e16649.

https://doi.org/10.1021/acssynbio.3c00684
ACS Synth. Biol. 2024, 13, 1467−1476